LAWRENCE
LIVERMORE
NATIONAL
LABORATORY

LLNL-PROC-406065

Crystallographic anisotropy of growth and etch rates of CVD diamond

M. Wolfer, J. Biener, B. S. El-dasher, M. M. Biener, A. V. Hamza, A. Kriele, C. Wild

August 6, 2008

19th European Conference on Diamond, Diamond-like Materials, Carbon Nanotubes, and Nitrides
Sitges, Spain
September 7, 2008 through September 11, 2008

Disclaimer

Crystallographic anisotropy of growth and etch rates of CVD diamond

Marco Wolfer[a], Jürgen Biener[b], Bassem S. El-dasher[b], Monika M. Biener[b], Alex V. Hamza[b], Armin Kriele[a], Christoph Wild[a]

[a]Fraunhofer-Institut für Angewandte Festkörperphysik, Tullastraße 72, 79108 Freiburg i. Br., Germany
[b]Lawrence Livermore National Laboratory, Livermore, California 94550, USA

Abstract

The investigation of orientation dependent crystal growth and etch processes can provide deep insights into the underlying mechanisms and thus helps to validate theoretical models. Here, we report on homoepitaxial diamond growth and oxygen etch experiments on polished, polycrystalline CVD diamond wafers by use of electron backscatter diffraction (EBSD) and white-light interferometry (WLI). Atomic force microscopy (AFM) was applied to provide additional atomic scale surface morphology information. The main advantage of using polycrystalline diamond substrates with almost random grain orientation is that it allows determining the orientation dependent growth (etch) rate for different orientations within one experiment. Specifically, we studied the effect of methane concentration on the diamond growth rate, using a microwave plasma CVD process. At 1 % methane concentration a maximum of the growth rate near <100> and a minimum near <111> is detected. Increasing the methane concentration up to 5 % shifts the maximum towards <110> while the minimum stays at <111>. Etch rate measurements in a microwave powered oxygen plasma reveal a pronounced maximum at <111>. We also made a first attempt to interpret our experimental data in terms of local micro-faceting of high-indexed planes.

Keywords: Diamond CVD, Homoepitaxy, Etching, Orientation

1. Introduction

Over the past 20 years, progress in the field of microwave plasma enhanced CVD (MPCVD) has led to the synthesis of high quality diamond [1-2], which forms the basis for a variety of applications [3]. Much effort has been devoted to the optimization of the growth of single diamond crystals [4-6] by controlling deposition parameters such as temperature, gas composition, and substrate orientation. The underlying growth processes have been studied by performing growth experiments on surfaces which are slightly misoriented from low index

planes [7-11]. However, a unifying atomic scale growth model explaining the observed growth kinetics on different diamond surface orientations is still missing. The purpose of the present work is to generate the experimental data necessary to develop a deeper understanding of the surface processes during diamond CVD.

A common crystallographic approach to obtain information about displacement velocities and growth morphologies of high-index crystal planes are sphere growth experiments. The idea is that an ideal crystal sphere exhibits all crystallographic faces equally and therefore supplies detailed information about the growth mechanisms. A successful diamond sphere growth experiment under CVD conditions published by van Enckevort et al. [12] showed that the surface processes of diamond growth depends strongly on substrate orientation. However, the preparation, characterization and handling of diamond spheres for growth rate experiments is challenging and makes systematic studies difficult.

Here, we describe the results of homoepitaxial growth and oxygen etch experiments on polished polycrystalline CVD diamond wafers. Our samples exhibit an almost random grain orientation similar to the situation in a sphere growth experiment, and thus allow us to obtain the complete orientational growth (etch) rate dependence within one experiment.

2. Experimental

Polycrystalline diamond samples with an average thickness of 250 µm were grown on <001> Si substrates, 25 mm in diameter and 5 mm in thickness, using an ellipsoidal microwave plasma reactor operated at 2.45 GHz microwave frequency [13]. The as-grown polycrystalline diamond surfaces were polished to a mirror-like surface finish with roughness values around 5 nm (rms). To facilitate the analysis of our growth experiments, we machined a grid of reference lines (1x1 mm^2 cell size) into the diamond surface using a Nd:YAG laser. Finally, the samples were carefully cleaned in acetone, isopropanol, rinsed with methanol and dried under a stream of dry nitrogen gas.

Using these samples as substrates, we then studied the effect of crystallographic surface orientation on both growth and etch rates of diamond using the following experimental procedure: First, we measured the surface topography and generated a grain orientation map of one of the 1x1 mm^2 cells using a combination of whitelight interferometry and electron backscatter diffraction (EBSD). This data set provides the baseline for the analysis of the following growth/etch experiments. Next, we deposited (or etched) a few hundred nm of diamond on (or from) the sample (5-15 min plasma exposure), and measured the surface topography of the same surface area again. To obtain the average growth/etch rate the surface

of the sample was partially masked by a thin sheet of polycrystalline diamond. Additional atomic scale information was obtained by atomic force microscopy (AFM). In order to correlate the grain orientation map (EBSD data) with the topographic (height) information obtained by whitelight interferometry we developed a computer program which automatically compensates for image distortions between the two data sets by using prominent surface features as landmarks. We then corrected the data for prior height differences between the surface grains caused by the anisotropic polishing behaviour of polycrystalline diamond. Finally, the grain orientation - growth (etch) rate correlation was visualized by plotting the data into a stereographic projection triangle in the form of circles. Here, the position of the circles indicates the grain orientation, their colour the grain height (relative growth rate) and their diameter the grain size. Specifically, we studied the effect of methane concentration (1-5% methane in hydrogen) of the growth kinetics using the following conditions: 300 sccm total flow rate, 150 mbar gas pressure, 6 kW microwave power, and substrate temperatures of 750-790 °C (measured by an optical pyrometer). Etching experiments with 2 % oxygen in hydrogen were performed in the same reactor under similar conditions.

3. Results and Discussion

3.1. Anisotropic abrasion resistance

In order to be able to analyze the growth (etch) experiments discussed in the following sections it is necessary to characterize the surface topography of our polished polycrystalline diamond substrates. A typical example of the surface topology is shown in Fig. 1. Already a simple visual comparison of this image with the corresponding EBSD grain orientation map shown in Fig. 2 reveals that grains with orientations near <111> stick out of the surface and therefore must have a higher abrasion resistance. Fig. 3 shows the computer analyzed correlation between the two data sets. A confined area of high grains (red circles) lies near the <111> corner of the stereographic triangle. Surfaces with orientations away from <111> direction are generally lower, i.e. they wear away faster during polishing, and there is an obvious difference in terms of inclination towards <101> and <001>. Grains along <111> - <001> line possess an intermediate wear resistance, whereas grains near the <101> corner are subject to stronger abrasion. These observations are in good agreement with our previous study [14] and can be explained on the basis of the periodic bond chain (PBC) vector model developed by van Bouwelen and van Enckevort [15].

3.2. Surface etching

Oxygen-plasma etching for 5 min resulted in a mean etch rate of 2.4 µm/h and a peak-to-valley ratio between highest and lowest grains of approximately 300 nm, compared to 100 nm of the polished surface prior to etching. Thus the anisotropic etch rate leads to considerable roughening of the surface even after removing as little as 200 nm of diamond. The orientation-height correlation of the etched surface is displayed in Fig. 4. Grains with orientations near the middle of the connection line of <101> and <001> exhibit a low removal rate, while planes near {111} are preferentially etched. These results are in accordance with former studies on single crystal diamond, though the oxygen treatment was done under different conditions [16-20].

A comparison of the AFM measurement is shown Fig. 5 with the corresponding EBSD map reveals the roughening of the fast etching (111) planes during the oxygen plasma treatment, while faces near (101) remain smooth and thus are etched via a layer-by-layer mechanism.

3.3. Crystallographic anisotropy of homoepitaxial growth

The orientation-height correlation obtained after 15 min of diamond growth at 1% methane is shown in Fig. 6. A mean growth rate of 0.8 µm/h was observed. Low, slow growing grains (blue circles) are clustered in the <111> corner of the stereographic triangle. A broad band of grains with medium growth rate extends from the <101> corner to the middle of the connection line between <001> and <111>. The maximum growth velocities can be found near the middle of the <101> - <001> connection.

Increasing the methane concentration to 3% leads to a different distribution (Fig. 7). In contrast to the deposition at 1% methane the mean growth rate increased by a factor of almost 4 (up to 3.2 µm/h). While the <111> growth direction is still the slowest, higher methane concentrations cause a strong increase in growth rate for grains located near the <001>-<101> side of the stereographic triangle.

Increasing the methane concentration to 5% further increases the average growth rate to 5.6 µm/h. Compared to the homoepitaxial growth at 3% methane the orientation-height correlation shown in Fig. 8 reveals distinct differences. The area of fastest growing grains (red circles) moved more towards <101> corner, and now covers a wider range of crystallographic orientations. Medium growth rates are now concentrated along the <111> - <001> side of the sterographic triangle, and the slowest growing grains are again found in the <111> corner.

3.4 Discussion and outlook

Micro-facetting of high index planes is one possibility to explain the observed growth rate anisotropy. In a first attempt to test this hypothesis we developed a computer algorithms that calculates the micro-faceting of high-index planes, i.e. the formation of local {100} and {111} faces covering the entire surface. From these simulations the relative contribution of {100} and {111} faces to the surface area and the density of step edges can be derived. An example showing the theoretical micro-facetting of a high-index plane is shown in Fig. 9. By correlating theoretical surface micro-topographies with experimental data we expect to obtain valuable information about growth and etching mechanisms for CVD diamond. These results will be published in a subsequent paper.

4. Conclusions

In the present work we have investigated the crystallographic anisotropy of homoepitaxial growth and oxygen etching of CVD diamond. For this purpose we combined orientational information obtained from electron backscatter diffraction (EBSD) with height information obtained by whitelight interferometry. Both etching and growth experiments result in pronounced changes of the surface morphology even after short exposure times. A preferred etching of (111) planes is observed while grains with orientations between <101> and <001> are much more resistant. Additional AFM measurements show that the <111> grains exhibit a rough surface. Growth experiments performed at three different methane concentrations reveal a pronounced dependence of the growth rate on the local orientation of the surface facet. Possible explanations based on the micro-facetting of high-index planes will be the subject of a forthcoming paper.

Acknowledgements

Part of this work was performed under the auspices of the U.S. Department of Energy by Lawrence Livermore National Laboratory under Contract DE-AC52-07NA27344.

References

[1] T. Teraji, Physica Status Solidi (a) 203, No 13, 2006 3324-3357

[2] J. Achard, F. Silva, A. Tallaire, X. Bonnin, G. Lombardi, K. Hassouni and A. Gicquel, J. Phys. D: Appl. Phys. 40 (2007) 6175-6188

[3] P. Koidl, C. Klages, Diamond and Related Materials 1 (1992) 1065

[4] A. Tallaire, J. Achard, F. Silva, R.S. Sussmann, A. Gicquel Diamond and Related Materials.14 (2005) 249-254

[5] M.G. Donato, G. Faggio, G. Messina, R. Potenza, S. Santangelo, M. Scoccia, C. Tuvé, G. Verona Rinati. Diamond and Related Materials 15 (2006) 517-521

[6] A. Chayahara, Y. Mokuno, Y. Horino, Y. Takasu, H. Kato, H. Yoshikawa, N. Fujimori, Diamond and Related Materials 13 (2004) 1954-1958

[7] T. Bauer, M. Schreck, H. Sternschulte, B. Stritzker, Diamond and Related Materials 14 (2005) 266-271

[8] H. Miyatake, K. Arima, O. Maida, T. Teraji, T. Ito, Diamond and Related Materials 16 (2007) 679-684

[9] N. Lee, A. Badzian, Diamond and Related Materials 6 (1997) 130-145

[10] W.J.P van Enckevort, G. Janssen, W. Vollenberg, L.J. Gilling, Journal of Crystal Growth 148 (1995) 365-382

[11] F. Silva, et al., Diamond and Related Materials (2008), doi: 10.1016/j.diamond.2008.01.006

[12] W.J.P van Enckevort, G. Janssen and L.J. Giling, Journal of Crystal Growth 113 (1991) 295-304

[13] M. Füner, C. Wild, P. Koidl, Appl. Phys. Lett. 72 (1998) 1149.

[14] B. S. El-Dasher, J. J. Gray, J. W. Tringe, J. Biener, A. V. Hamza, C. Wild, E. Wörner, P. Koidl, Applied Physics Letters 88 (2006) 241915

[15] F. M. van Bouwelen, W.J.P. van Enckevort, Diamond and Related Materials 8 (1999) 840-844

[16] W.J.P. van Enckevort and F.K. de Theije, in "Properties, Growth and Applications of Diamond", M.H. Nazaré and A.J. Neves, Eds. (Inspec, London, 2001) pp115-124

[17] J.E. Field, Properties of Diamond, Academic Press, 1979

[18] F.K. de Theije, O. Roy, N. J. van der Laag, W.J.P van Enckevort, Diamond and Related Materials 9 (2000) 929-934

[19] S. Dallek, L. Kabacoff and M. Norr, Thermochimica Acta, 192 (1991) 321-326

[20] Q. Sun and M. Alam, J. Electrochemi. Soc., Vol 139, No. 3 (1992)

[21] C. Wild, P. Koidl, W. Müller-Sebert, H. Walcher, R. Kohl, N. Herres, R. Locher, R. Salemski und R. Brenn. Diamond and Related Materials, 3:373, 1994.

Legends

Figure1: Topography of a specimen obtained by whitelight interferometry after polishing. High grains, i.e. grains with a high abrasion resistance, are coloured red, low grains blue.

Figure2: a) EBSD map of the same surface area as in Fig. 1. b) IPF plot showing the orientation distribution as a function of multiples of random distribution (MRD). c) Correlation between colour and orientation for picture a).

Figure3: A typical orientation height correlation after polishing. The position of the circles in the stereographic triangle corresponds to the crystallographic orientation of the grains, the colour to their relative height.

Figure4: Orientation height correlation after 5 min oxygen plasma treatment.

Figure5: AFM measurement of the specimens surface after 5 min oxygen plasma treatment.

Figure6: Orientation height correlation after 15 min growth under 1% methane.

Figure7: Orientation height correlation after 15 min growth under 3% methane.

Figure8: Orientation height correlation after 15 min growth under 5% methane.

Figure9: Simulated micro-faceting of a high-index face with (10,5,2) orientation. The {100} facet is blue, the two {111} facets are coloured pink.

Figure 1

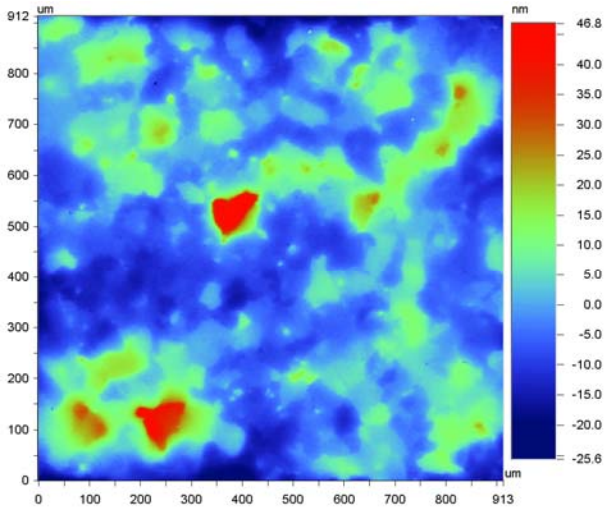

Figure 2

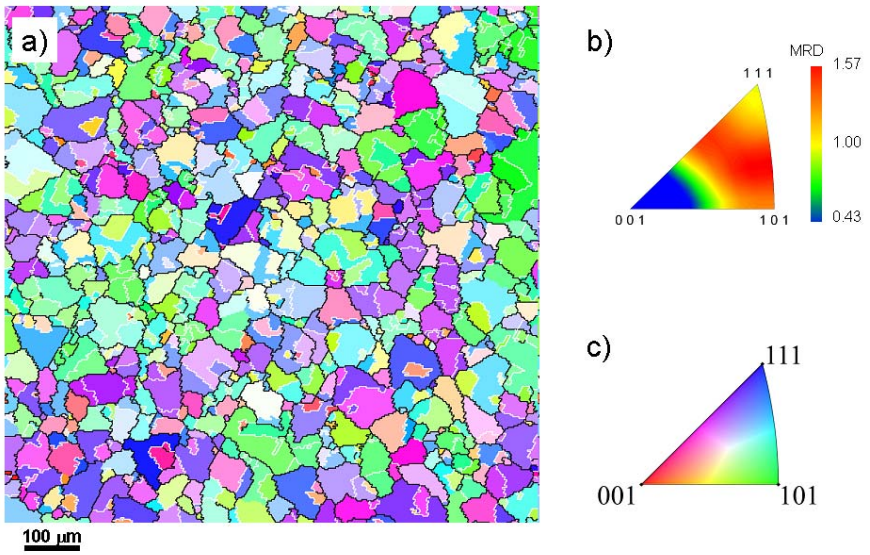

Figure 3

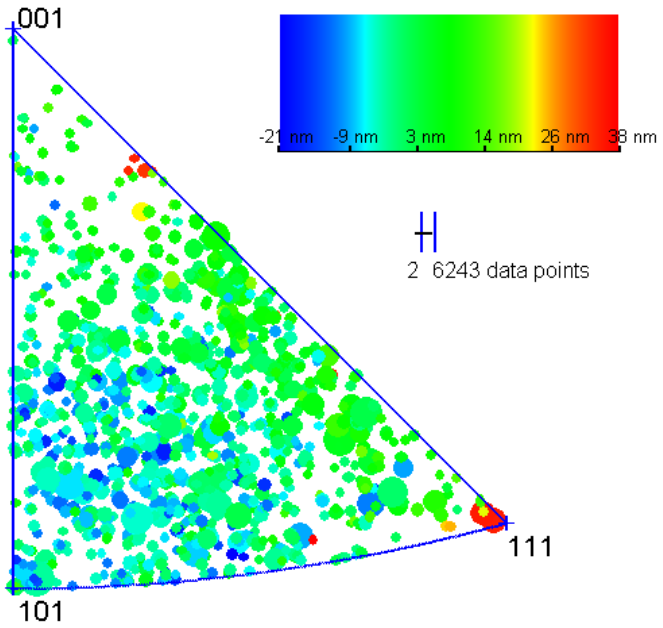

Figure 4

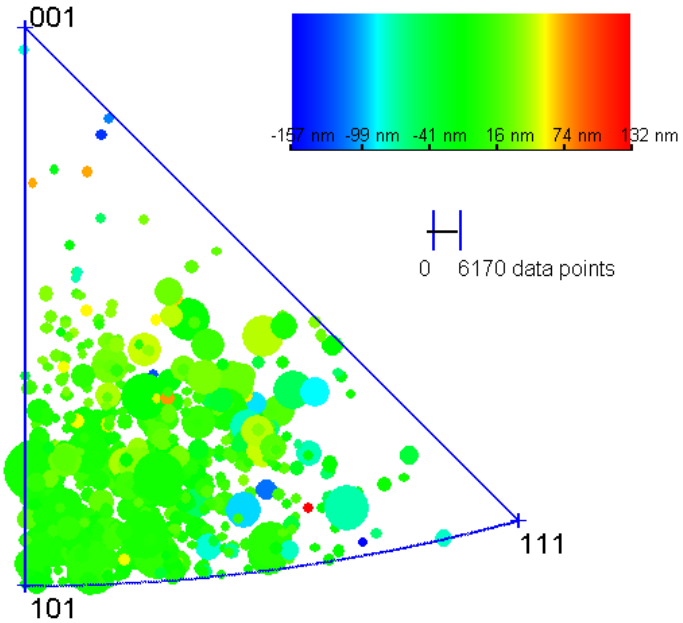

Figure 5

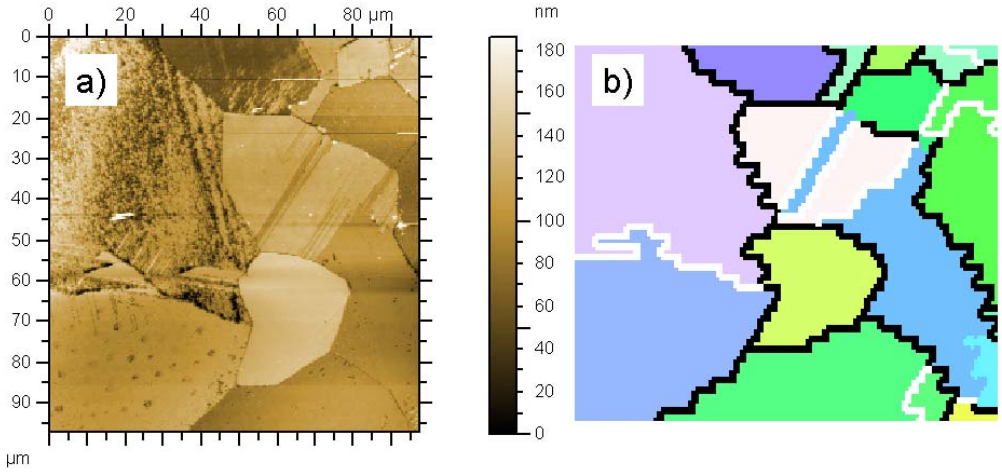

Figure 6

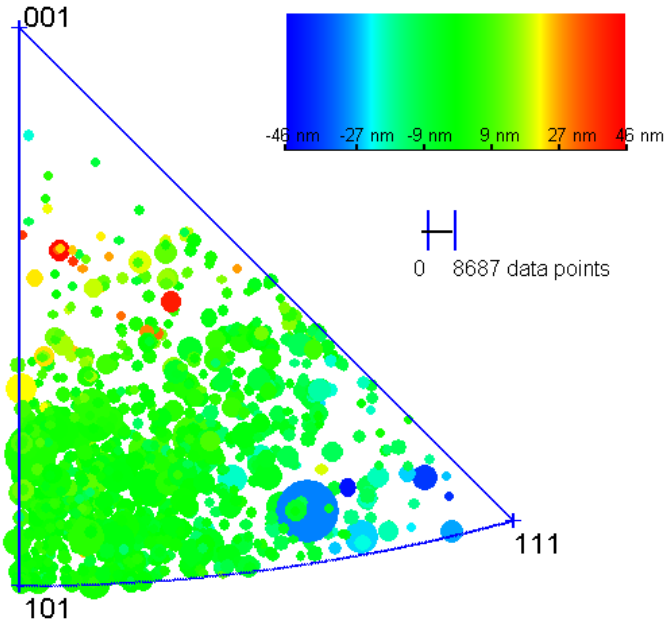

Figure 7

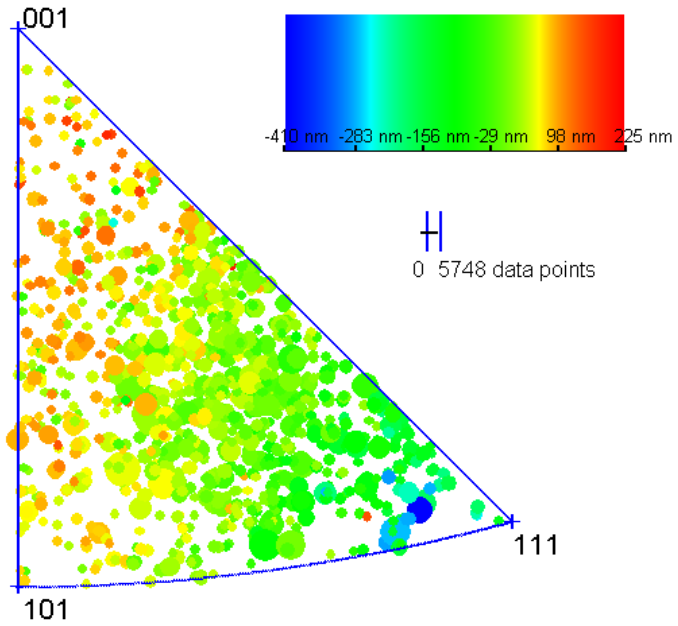

Figure 8

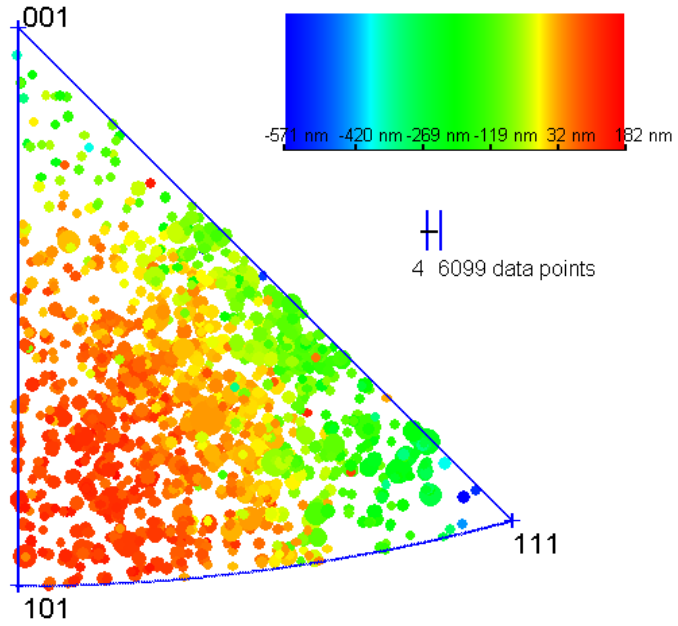

Figure 9

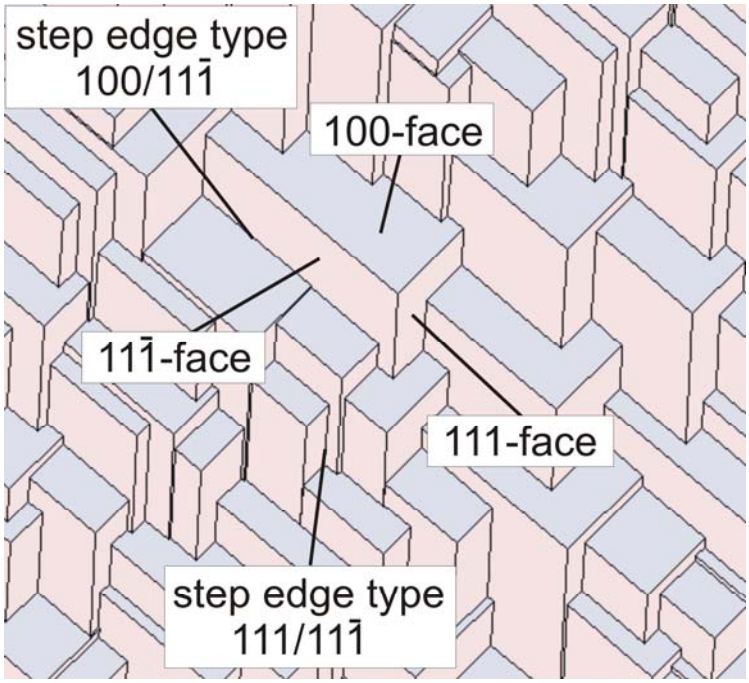
step edge type
100/11$\bar{1}$
100-face
11$\bar{1}$-face
111-face
step edge type
111/11$\bar{1}$